Stress-Strain Characteristics of Clay Brick Masonry under Uniaxial Compression

Hemant B. Kaushik[1]; Durgesh C. Rai[2]; and Sudhir K. Jain, M.ASCE[3]

Abstract: The uniaxial monotonic compressive stress-strain behavior and other characteristics of unreinforced masonry and its constituents, i.e., solid clay bricks and mortar, have been studied by several laboratory tests. Based on the results and observations of the comprehensive experimental study, nonlinear stress-strain curves have been obtained for bricks, mortar, and masonry and six "control points" have been identified on the stress-strain curves of masonry, which can also be used to define the performance limit states of the masonry material or member. Using linear regression analysis, a simple analytical model has been proposed for obtaining the stress-strain curves for masonry that can be used in the analysis and design procedures. The model requires only the compressive strengths of bricks and mortar as input data, which can be easily obtained experimentally and also are generally available in codes. Simple relationships have been identified for obtaining the modulus of elasticity of bricks, mortar, and masonry from their corresponding compressive strengths. It was observed that for the strong and stiff bricks and mortar of lesser but comparable strength and stiffness, the stress-strain curves of masonry do not necessarily fall in between those of bricks and mortar.

DOI: 10.1061/(ASCE)0899-1561(2007)19:9(728)

CE Database subject headings: Bricks; Brick masonry; Mortars; Compressive strength; Stress strain relations; Regression analysis.

Introduction

Masonry walls are used in almost all types of building construction in many parts of the world because of low cost material, good sound and heat insulation properties, easy availability, and locally available material and skilled labor. Mathematical modeling of structures with masonry walls requires the material properties and constitutive relationships of masonry and its constituents, i.e., bricks and mortar, which are not easily available because of scarcity of controlled experimental tests and significant variation in material properties geographically.

The paper is concerned with the uniaxial monotonic compressive stress-strain behavior and other characteristics of local hand molded burnt clay solid bricks, mortar, and unreinforced masonry prisms. In the comprehensive experimental study, tests were performed on 40 brick specimens manufactured by four different kilns, 27 mortar cube specimens of three different grades, and 84 specimens of masonry prisms (combination of four bricks and three mortar types). In addition, initial rate of absorption (IRA) and water absorption (WA) of bricks were determined by standard tests. Based on the experimental results and observations, stress-strain curves have been developed for bricks, mortar, and masonry and simple relations have been suggested for estimation of modulus of elasticity of bricks, mortar, and masonry from their corresponding compressive strengths. A simple analytical model has been proposed for obtaining the nonlinear stress-strain curves of masonry, which is a function of only the compressive strengths of bricks and mortar cubes. The model is based on six "control points" on the stress-strain curves, which can be effectively used to define the performance limit states of the masonry material or member.

Compressive Behavior of Masonry

Masonry is typically a nonelastic, nonhomogeneous, and anisotropic material composed of two materials of quite different properties: stiffer bricks and relatively softer mortar. Under lateral loads, masonry does not behave elastically even in the range of small deformations. Masonry is very weak in tension because it is composed of two different materials distributed at regular intervals and the bond between them is weak. Therefore, masonry is normally provided and expected to resist only the compressive forces. As shown in Figs. 1(a and b), during compression of masonry prisms constructed with stronger and stiffer bricks, mortar of the bed joint has a tendency to expand laterally more than the bricks because of lesser stiffness. However, mortar is confined laterally at the brick–mortar interface by the bricks because of the bond between them; therefore, shear stresses at the brick-mortar interface result in an internal state of stress which consists of triaxial compression in mortar and bilateral tension coupled with axial compression in bricks. This state of stress initiates vertical splitting cracks in bricks that lead to the failure of the prisms (McNary and Abrams 1985; Atkinson and Noland 1983; Drysdale et al. 1994).

[1]Ph.D. Scholar, Dept. of Civil Engineering, Indian Institute of Technology Kanpur, Kanpur 208 016, India. E-mail: hemantbk@gmail.com

[2]Associate Professor, Dept. of Civil Engineering, Indian Institute of Technology Kanpur, Kanpur 208 016, India (corresponding author). E-mail: dcrai@iitk.ac.in

[3]Professor, Dept. of Civil Engineering, Indian Institute of Technology Kanpur, Kanpur 208 016, India. E-mail: skjain@iitk.ac.in

Note. Associate Editor: Chiara F. Ferraris. Discussion open until February 1, 2008. Separate discussions must be submitted for individual papers. To extend the closing date by one month, a written request must be filed with the ASCE Managing Editor. The manuscript for this paper was submitted for review and possible publication on November 20, 2005; approved on January 31, 2006. This paper is part of the ***Journal of Materials in Civil Engineering***, Vol. 19, No. 9, September 1, 2007. ©ASCE, ISSN 0899-1561/2007/9-728–739/$25.00.

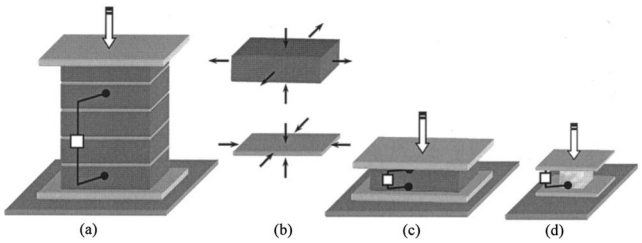

Fig. 1. Test setup for different specimens: (a) masonry prism; (b) triaxial state of stress at interface of brick and mortar in masonry prism; (c) brick unit; and (d) mortar cube

Since masonry is an assemblage of bricks and mortar, it is generally believed that the strength and stiffness of masonry would lie somewhere between that of bricks and mortar. It may be true in cases when one component of masonry, i.e., either bricks or mortar, is substantially weaker and softer than the other, for example, bricks found in the southern part of India are very weak and soft as reported by Dayaratnam (1987) and Sarangapani et al. (2002). Based on an experimental study, Sarangapani et al. (2002) reported that soft bricks (modulus of elasticity ~500 MPa) were responsible for development of triaxial compression in bricks and axial compression with lateral tension in mortar joints of masonry prism. This behavior is contradictory to the generally accepted behavior of the masonry constructed with stiff bricks and softer mortar.

Sarangapani et al. (2005) conducted a series of tests on masonry prisms constructed with very soft bricks (modulus of elasticity ~500 MPa) and a combination of different mortar grades. It was observed that for the soft brick-stiff mortar masonry, the compressive strength of masonry increases with the increase in bond strength, which increases with the mortar strength along with other factors. Ewing and Kowalsky (2004) tested three unconfined and ungrouted single-wythe clay brick masonry prisms constructed with single brick type and mortar grade and proposed four performance limit states, which correspond to 75 and 90% of prism compressive strength on the rising part of stress-strain curve and 50 and 20% of prism compressive strength on the falling branch. It was concluded that the stress-strain curve of masonry can be adequately predicted by the "modified" Kent–Park model proposed for concrete masonry by Priestley and Elder (1983). The "modified" Kent–Park model (Priestley and Elder 1983) was also justified by Paulay and Priestley (1992) for use in case of unconfined masonry. The model consists of three portions: a parabolic rising curve, a linear falling branch, and a final horizontal plateau of constant stress (at 20% of masonry prism strength), which are defined by the following equations

$$f_m = 1.067 f'_m \left[\frac{2\varepsilon_m}{0.002} - \left(\frac{\varepsilon_m}{0.002} \right)^2 \right] \quad \text{for } 0 \leq \varepsilon_m \leq 0.0015 \text{ (rising curve)} \tag{1}$$

$$f_m = f'_m[1 - Z_m(\varepsilon_m - 0.0015)] \text{ until } 0.2 f'_m \text{ (descending curve)} \tag{2}$$

where

$$Z_m = \frac{0.5}{\left[\frac{3 + 0.29 f_j}{145 f_j - 1000} \right] - 0.002} \tag{3}$$

f_m and ε_m=compressive stress and strain in masonry; f'_m=compressive prism strength of masonry; and f_j=compressive strength of mortar. However, Priestley and Elder (1983) did not suggest any method to estimate f'_m to be used in the above equations.

McNary and Abrams (1985) conducted several uniaxial, biaxial, and triaxial tests on clay bricks, mortar, and masonry to validate an analytical model describing the failure criteria of masonry prisms, which considers the nonlinear behavior of confined mortar (between bricks) and splitting strengths of bricks. It was observed that the failure of masonry prisms took place because of lateral tensile splitting of bricks, which was induced in the bricks by the mortar. Several relations were proposed for the analytical determination of compressive strengths of bricks, mortar, and masonry, which depend upon their compressive and tensile strengths.

By regression analysis of several experimental results on hollow structural clay tiles, Bennett et al. (1997) showed that the masonry prism strength has a linear relationship with the compressive strength of bricks, and that the prism strength for loading perpendicular to the bed joint can be conservatively estimated as three-tenths of the brick compressive strength. This method of estimating the masonry prism strength may overestimate the prism strength because it does not give any weightage to the strength of mortar used in prisms. Also, a linear relationship was proposed between elastic modulus and prism strength of masonry. Sawko and Rouf (1984) presented an analytical approach for the calculation of axial and bending stiffness of masonry walls by considering parabolic variation of stress-strain curves for masonry in compression based on past experimental studies. The parabolic variation was proposed to continue in the descending part until 1.5 times the peak strain corresponding to prism strength is reached, however, the authors did not suggest any method of estimating the peak strain.

Using experimental data, Grimm (1975), Paulay and Priestley (1992), and Binda et al. (1988) suggested several analytical relations for estimation of strength and deformation characteristics of masonry, which depend upon the compressive and tensile strengths of bricks and mortar along with several other factors.

Although a large number of tests have been conducted in the past on masonry and its constituents, very few studies have actually suggested simple analytical relations to determine the compressive strength and deformation characteristics of masonry (Grimm 1975; McNary and Abrams 1985; Paulay and Priestley 1992; Bennett et al. 1997). A few analytical models have also been developed to plot the compressive stress-strain curves for masonry (Priestley and Elder 1983; Sawko and Rouf 1984; McNary and Abrams 1985; Paulay and Priestley 1992; Ewing and Kowalsky 2004). However, most of these analytical relations and models are too complicated and require a lot of experimental data pertaining to both compressive and tensile behavior of bricks, mortar, and masonry. This emphasizes the importance of conducting more tests on compressive behavior of masonry and its constituents, and further to develop simple analytical equations to determine the compressive strength and deformation characteristics of masonry, which can be used in the analysis and design procedure.

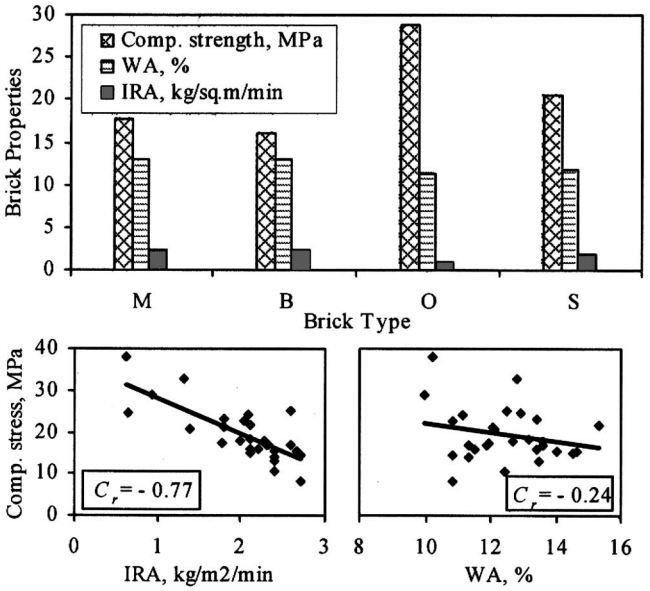

Fig. 2. Effect of water absorption and initial rate of absorption on compressive strength of bricks (C_r=correlation coefficient)

Experimental Program

Several tests were carried out in order to evaluate the uniaxial compressive stress-strain curves of brick units, mortar cubes, and masonry prisms constructed with different combinations of bricks and mortar grades. Local bricks from four different manufacturers (designated as M, B, S, and O) were used, having approximate length, width, and height as 230, 110, and 75 mm, respectively. IRA and WA tests were performed on brick units to get information about the quality of bricks. Masonry prisms and mortar cubes were subjected to monotonically increasing displacement loading (strain controlled) at their top which was applied vertically by a 250 kN load and ±125 mm displacement capacity MTS servo-hydraulic actuator. However, brick units were tested in a 2,000 kN universal testing machine under stress-controlled loading.

Each specimen was instrumented with an Epsilon extensometer to record the displacement response during the tests. Two sizes of extensometers were used in the study—a bigger one with gauge length of 200 nm and ±12 mm peak displacement capacity was used in prism testing and a smaller one with gauge length of 25 mm and ±5 mm peak displacement capacity was used in brick and mortar cube testing. In masonry prisms the displacement was recorded across three mortar joints as shown in Fig. 1(a) to include the deformations in bricks and mortar joints in the total deformation. In the case of brick units and mortar cubes, the displacements were recorded on their faces as shown in Figs. 1(c and d). The vertical load and displacement readings at specified locations in all the tests were directly recorded using a computer-based data acquisition system.

Stress-strain curves reported in the paper are arrived at by the double averaging method, i.e., averaged strain values are plotted on the abscissa against the predetermined stress values on the ordinate (control points), which are also averaged across different specimens. The highest and lowest values in a set of data are not considered while averaging that particular set of data. Modulus of elasticity is calculated from stress-strain curves by measuring the slope of a secant between ordinates corresponding to 5 and 33% of the ultimate strength of the specimens (MSJC 2002).

Tests for WA and IRA of Bricks

Total water absorption capacity of the brick material is given by the WA test. The absorption of moisture by capillary action in the bricks produces a *suction* effect that draws water from mortar and this characteristic is defined by IRA. The rate of absorption can have an important effect on the interaction between freshly laid mortar and the brick units. IRA is measured in order to assist in mortar selection and material handling in the construction process. It is measured in terms of mass of water absorbed (per minute) by the brick material per unit area of brick immersed in about 3 mm deep water, which is kept constant by adding water during the test, as per ASTM C 67-00 (ASTM 2001c). IS 3495 (IS 1992b) was used to perform a WA test whose provisions are similar to those given in ASTM C 67-00 (ASTM 2001c).

Fig. 2 shows the variation in compressive strength of bricks (f_b) with IRA and WA and Table 1 gives the corresponding statistics. WA was found to vary from 11 to 13% [mean 12.3%, coefficient of variation (COV) 0.13] and IRA varied from 0.97 to 2.42 kg/m^2/min (mean 1.9 kg/m^2/min, COV 0.34); lower IRA values were found for bricks with higher f_b. In the present study, a much better correlation was observed between IRA and f_b (correlation coefficient −0.77) than that between WA and f_b (correlation coefficient −0.24). Too high or too low an IRA is detrimental to achieving a good initial and final bond between brick and mortar, which not only affects the masonry flexural strength, but also its water tightness and durability. It was observed by Drysdale et al. (1994) that if IRA is less than 0.25 kg/m^2/min, which is a case for low absorption or low-suction bricks, then such bricks may tend to flow on mortar, particularly if the bricks are damp. On the other hand, for highly porous and absorptive bricks (IRA > 1.5 kg/m^2/min), a poor brick–mortar bond may result for thin mortar joints with less water–cement ratio because of rapid suction of water in mortar by bricks.

Stress-Strain Curves for Bricks

The tests were performed in accordance with ASTM C 67-00 (ASTM 2001c) and IS 3495 (IS 1992a). The experimental setup

Table 1. Summary of Test Results for Brick Units

Brick type	f_b (MPa)	Failure strain	E_b (MPa)	WA (%)	IRA (kg/m^2/min)
M (10 specimens)	17.7 [0.23][a]	0.0072 [0.18]	5,300 [0.15]	12.9 [0.11]	2.26 [0.12]
B (10 specimens)	16.1 [0.08]	0.0060 [0.19]	5,030 [0.34]	13.0 [0.11]	2.42 [0.09]
O (10 specimens)	28.9 [0.23]	0.0070 [0.39]	7,516 [0.26]	11.4 [0.21]	0.97 [0.34]
S (10 specimens)	20.6 [0.17]	0.0057 [0.28]	6,534 [0.10]	11.8 [0.05]	1.89 [0.24]
Average (40 specimens)	20.8 [0.33]	0.0065 [0.34]	6,095 [0.29]	12.3 [0.13]	1.90 [0.34]

[a]Figures in [ ] brackets indicate coefficient of variation.

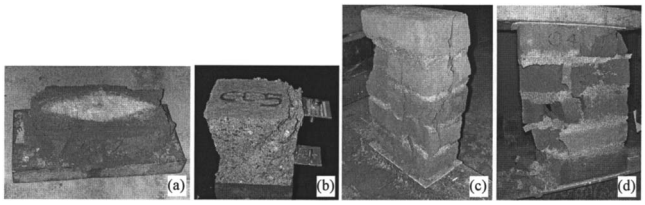

Fig. 3. Typical failure modes of: (a) brick units; (b) mortar cubes; and (c), (d) masonry prisms

for testing and the characteristic crushing failure of bricks is shown in Figs. 1(c) and 3(a), respectively. Fig. 4(a) shows the stress-strain curves for the four types of bricks obtained by averaging the stress-strain data from ten samples of each type of brick. The bricks were found to be behaving linearly up to about one-third of the ultimate failure load after which the behavior became highly nonlinear. An average stress-strain curve for all the brick types used in the study is also shown in Fig. 4(a). The summary of results including f_b, failure strains, and modulus of elasticity (E_b) are given in Table 1. For different bricks used in the study, mean values of f_b varied from 16.1 to 28.9 MPa (mean 20.8 MPa, COV 0.33). Mean values of failure strain recorded in the brick specimens were found to vary between 0.0057 and 0.0072 (mean 0.0065, COV 0.34) and E_b was found to vary between 5,000 and 7,500 MPa (mean 6,095 MPa, COV 0.29). Variation of E_b with f_b is shown in Fig. 5(a), and it is seen that E_b varies between 150 and 500 times f_b. An average value of E_b may be determined by

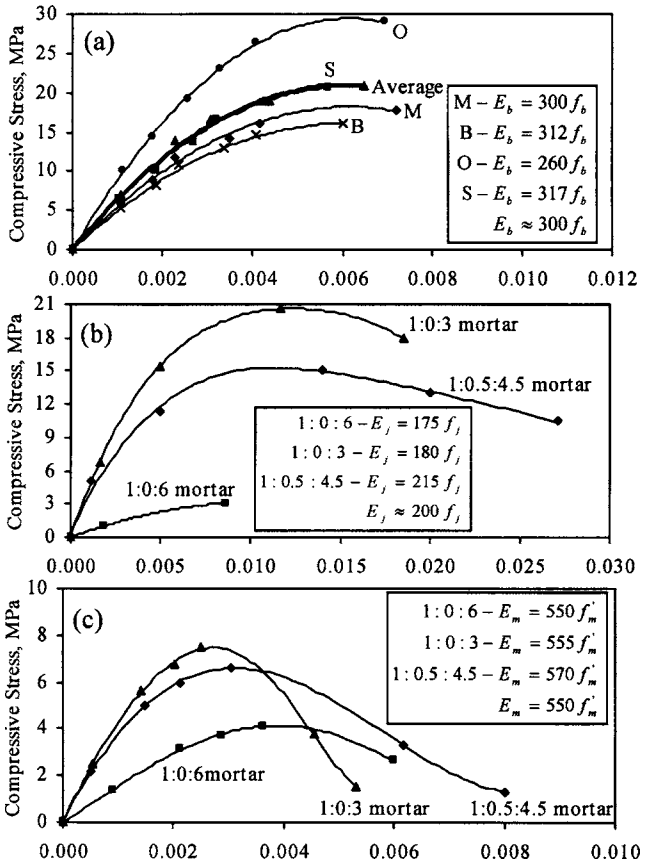

Fig. 4. Compressive stress-strain curves for: (a) brick units; (b) mortar cubes; and (c) masonry prisms

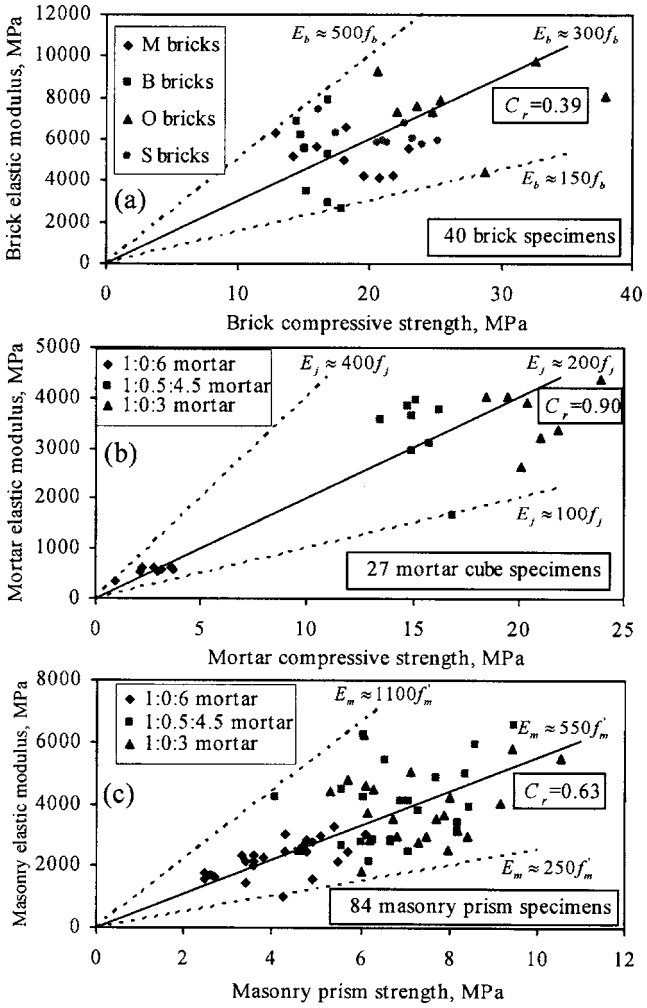

Fig. 5. Variation of modulus of elasticity of: (a) bricks; (b) mortar; and (c) masonry with corresponding compressive strengths

$$E_b \approx 300 f_b; \quad \text{(COV 0.35)} \tag{4}$$

E_b and f_b are not very well correlated as evident from significant scattering of data in Fig. 5(a); the coefficient of correlation, C_r=0.39; therefore Eq. (4) should be used with caution.

Stress-Strain Curves for Mortar Cubes

Three different grades of mortar (cement:lime:sand by volume) were used in the study, viz., 1:0:6 (*weak*), 1:0:3 (*strong*), and 1:0.5:4.5 (*intermediate*) and mortar cubes of 50 mm size were tested after 28 days of casting to obtain their compressive stress-strain curves. The procedure for obtaining the compressive strength of mortar cubes is given in ASTM C 109/C 109M-99 (ASTM 2001a) and IS 2250 (IS 1995). Experimental setup and typical failure of mortar cubes are shown in Figs. 1(d) and 3(b), respectively. Compressive strength of mortar depends upon the water–cement ratio and cement content. Water–cement ratio required for preparation of mortar was strictly monitored even though not controlled, and it was observed that the ratio varied from 0.7 to 0.8 for various mixes to obtain workable mortar in a very hot and dry climate (about 45 °C). Fig. 4(b) shows the compressive stress-strain curves for the three grades of mortar obtained by averaging the data from nine specimens of each grade. Initial straight portion of the stress-strain curve (up to about one-

Table 2. Summary of Test Results for Mortar Cubes

f_j (MPa)	Failure strain	E_j (MPa)
(a) *Weak* mortar—1:0:6 (9 specimens)		
3.1 [0.22]	0.0087 [0.38]	545 [0.30]
(b) *Strong* mortar—1:0:3 (9 specimens)		
20.6 [0.08]	0.0185 [0.21]	3,750 [0.16]
(c) *Intermediate* mortar—1:0.5:4.5 (9 specimens)		
15.2 [0.06]	0.0270 [0.36]	3,300 [0.26]

third of mortar strength) is followed by a nonlinear curve, which extends well beyond the strain limits corresponding to the brick samples. Strain readings on the falling branch of the stress-strain curve could not be recorded for the *weak* mortar because of its brittle and explosive crushing failure after reaching the ultimate strength. The crushing failure of two other mortar grade specimens was more ductile and nonexplosive. Mortar strength (f_j), failure strains, and modulus of elasticity (E_j) of mortar specimens are shown in Table 2.

Weak mortar was found to be very weak and soft as compared to the other two grades with mean f_j and E_j of only 3.1 MPa (COV 0.22) and 545 MPa (COV 0.30), respectively. On the other hand, mean f_j for *strong* and *intermediate* mortar was 20.6 MPa (COV 0.08) and 15.2 MPa (COV 0.06), respectively; and mean E_j was 3,750 MPa (COV 0.16) and 3,300 MPa (COV 0.26), respectively. Similarly, mean values of the failure strain at failure in *weak* mortar was only 0.0087 (COV 0.38) as compared to the values of 0.0185 (COV 0.21) and 0.027 (COV 0.36) for the *strong* and *intermediate* mortar, respectively. Fig. 5(b) shows that E_j varies between 100 and 400 times f_j and average value may be determined by

$$E_j \approx 200 f_j; \quad \text{(COV 0.32)} \tag{5}$$

For the present data, a very good coefficient of correlation (C_r=0.90) was observed between the experimentally observed E_j values and the values estimated using Eq. (5).

Intermediate mortar performed well in terms of strength and ductility as compared to the other two grades because of the presence of lime; f_j for *intermediate* mortar was about 35% less than that of *strong* mortar; however failure strain was about 45% more [Fig. 4(b)].

Stress-Strain Curves for Masonry Prism

Masonry prisms were constructed using combinations of four brick types and three mortar grades, and stress-strain curves were obtained by averaging the data from seven specimens of each combination. Approximate height of five-brick high masonry prism with 10-mm-thick mortar joints was about 400 mm. Compression testing was done following ASTM C 1314-00a (ASTM 2001b) and IS 1905 (IS 1987). General test setup and typical failure of masonry prisms are shown in Figs. 1(a) and 3(c and d), respectively. The stress-strain curves for masonry prisms are shown in Fig. 4(c) and the summary of results including prism strength (f'_m), failure strain, and modulus of elasticity (E_m) are given in Table 3. Failure of the majority of the prism specimens was due to the formation of vertical splitting cracks along their height. Failure of about 10–20% of specimens in each set took place because of crushing of an *odd* weaker brick in the prism or bond failure by flexural bending of specimens, probably due to "poor" alignment of the specimen with the loading arm of actuator; these results have not been included in the study.

Table 3. Summary of Test Results for Masonry Prisms

Brick type	f'_m (MPa)	Failure strain	E_m (MPa)
(a) Prisms with *weak* mortar—1:0:6 (4×7 specimens)			
M	4.0 [0.13]	0.0052 [0.53]	2,239 [0.30]
B	2.9 [0.17]	0.0034 [0.45]	1,795 [0.17]
O	5.1 [0.16]	0.0086 [0.15]	2,630 [0.14]
S	4.3 [0.17]	0.0065 [0.14]	2,355 [0.19]
Average	4.1 [0.24]	0.0059 [0.43]	2,300 [0.24]
(b) Prisms with *strong* mortar—1:0:3 (4×7 specimens)			
M	7.4 [0.10]	0.0067 [0.28]	3,585 [0.18]
B	6.5 [0.14]	0.0041 [0.39]	3,592 [0.25]
O	8.5 [0.21]	0.0057 [0.36]	5,219 [0.50]
S	7.6 [0.17]	0.0050 [0.55]	4,250 [0.44]
Average	7.5 [0.18]	0.0053 [0.41]	4,200 [0.38]
(c) Prisms with *intermediate* mortar—1:0.5:4.5 (4×7 specimens)			
M	6.5 [0.19]	0.0102 [0.17]	3,542 [0.27]
B	5.9 [0.23]	0.0062 [0.40]	3,509 [0.49]
O	7.2 [0.24]	0.0092 [0.32]	4,712 [0.33]
S	6.8 [0.23]	0.0066 [0.31]	3,325 [0.26]
Average	6.6 [0.20]	0.0080 [0.34]	3,800 [0.35]

Mean value of f'_m was found to be 4.1 MPa (COV 0.24), 7.5 MPa (COV 0.18), and 6.6 MPa (COV 0.20) for prisms constructed with *weak, strong*, and *intermediate* mortar, respectively. Mean failure strain was 0.0059 (COV 0.43), 0.0053 (COV 0.41), and 0.008 (COV 0.34) for masonry with *weak, strong*, and *intermediate* mortar, respectively. Masonry prisms constructed with *weak* mortar were found to be weaker and softer with mean E_m of 2,300 MPa (COV 0.24) as compared to those constructed with *strong* and *intermediate* mortar with mean E_m of 4,200 MPa (COV 0.38) and 3,800 MPa (COV 0.35), respectively. The stress-strain curve was found to be linear for up to about one-third of f'_m after which cracks began to form in the bricks introducing the nonlinearity. Fig. 5(c) shows that E_m varies between 250 and 1,100 times f'_m, and an average value of E_m may be determined by

$$E_m \approx 550 f'_m; \quad \text{(COV 0.30)} \tag{6}$$

For the present data, a relatively good coefficient of correlation (C_r=0.63) was observed between the experimentally observed E_m values and the values estimated using Eq. (6), which was found to be in line with internationally accepted documents and codes, e.g., FEMA306 (FEMA 1999), which also proposes $E_m \approx 550 f'_m$. International Building Code (IBC 2003) and the MSJC document (MSJC 2002) recommend E_m as 700 times f'_m, while Paulay and Priestley (1992) and Eurocode6 (CEN 1996) suggest conservatively higher values of E_m (750 and 1,000 times f'_m, respectively). The Canadian masonry code S304.1 (CSA 2004) recommends E_m as 850 times f'_m with an upper limit of 20,000 MPa. Drysdale et al. (1994) plotted E_m and f'_m obtained from past experimental studies and showed that E_m varies from 210 to 1,670 times f'_m.

Fig. 4(c) shows that the behavior of masonry prisms constructed using *strong* and *intermediate* mortar was quite similar in the linear region, while the best performance was shown by prisms with *intermediate* mortar, which has lime content (C:L:S=1:0.5:4.5). Although, f'_m was found to be about 13%

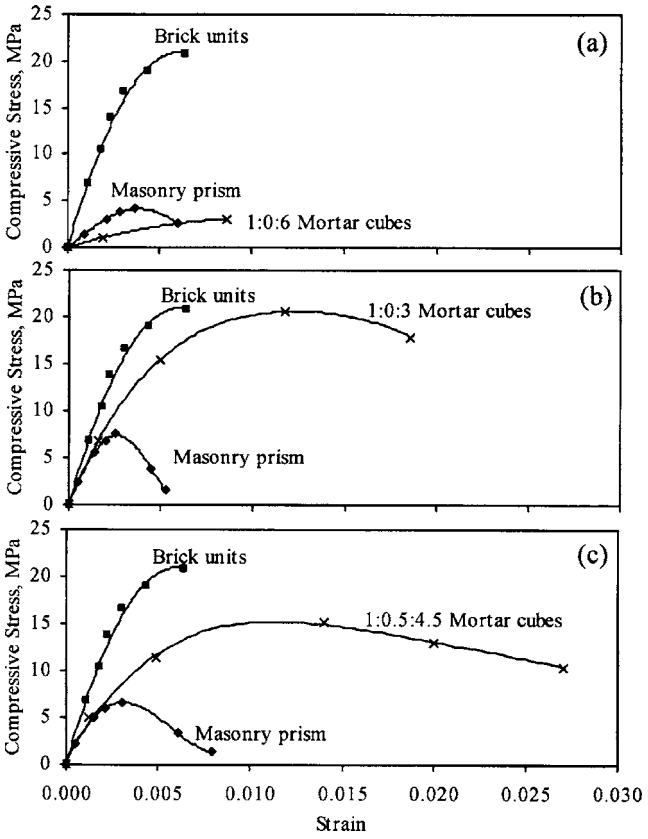

Fig. 6. Comparison of stress-strain curves for brick units, mortar cubes, and masonry prisms for different grades of mortar: (a) *weak*; (b) *strong*; and (c) *intermediate*. (Data points represent experimental results and solid lines represent corresponding trend lines.)

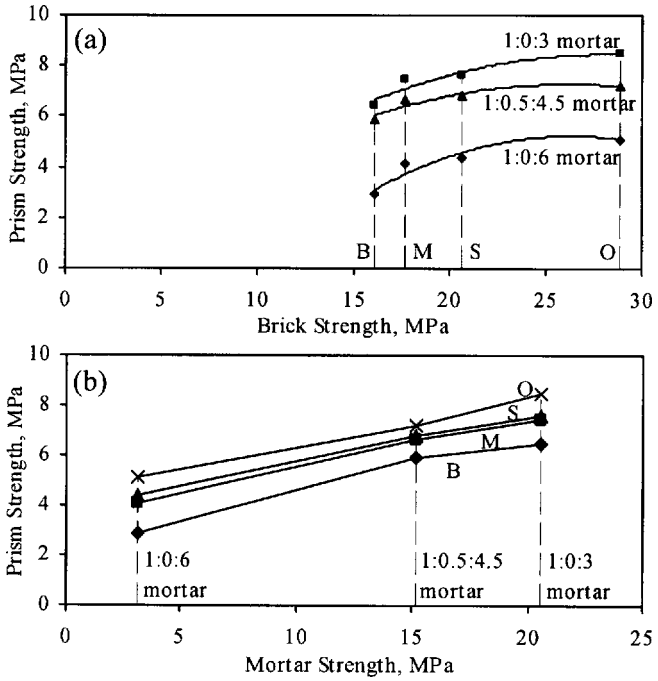

Fig. 7. Relationship between: (a) masonry prism strength and brick compressive strength for different mortar grades; (b) masonry prism strength and mortar compressive strength for different bricks

less for prisms with *intermediate* mortar than those with *strong* mortar, the failure strain was about 50% more. Thus, there is a significant improvement in the ductility of masonry in compression without any considerable compromise with the compressive strength because of lime in mortar. Therefore, the age-old practice of using lime in mortar, which has been discontinued in many parts of the world for various reasons, appears to have a role in improving performance and its use should be required.

Fig. 6 and Tables 1 and 2 show that a majority of the bricks used in the present study were stronger and stiffer than the mortar used. Fig. 6(a) shows that the stress-strain curves of masonry constructed with *weak* mortar falls in between those of bricks and mortar. On the other hand, for masonry constructed with *intermediate* and *strong* mortar [Figs. 6(b and c)], the stress-strain curves of masonry fall on the lower side of those corresponding to bricks and mortar. Therefore, the generally believed *go-between* compressive behavior of masonry may not be applicable for all the cases, especially when the strength and stiffness of bricks and mortar are comparable.

Figs. 7(a and b) show that f'_m increases with f_b and f_j for all the brick types and all the mortar grades, however the increase is more prominent when weaker mortar is used in constructing masonry. This characteristic behavior of masonry has also been reported in past studies (Drysdale et al. 1994). Therefore, although some minimum strength of mortar is required for strength and to ensure adequate durability, other considerations such as better workability of the fresh mortar and a more deformable mortar to accommodate differential movements have led to the common advice of not using a higher strength mortar than is required for the job.

Control Points Defining Stress-Strain Curves of Masonry

Based on the limit states proposed by Ewing and Kowalsky (2004), six control points were identified on the stress-strain curves of masonry in the present study, which correspond to the experimentally observed six *significant* events representing compressive stresses in masonry and the corresponding compressive strains. The six control points represent 33, 75, 90, and 100% of f'_m on the rising part, and 50 and 20% of f'_m on the falling branch of stress-strain curve as shown in Fig. 8. Strain values used to define the control points depend largely upon the mortar grade used in prisms. In the case of prisms constructed with *weak* mortar, strain readings in the descending part of the curve could not be recorded after the compressive stress reduced to about 60% of f'_m after reaching peak because of brick–mortar bond failure in most of the cases, and sudden and brittle failure of the specimens. The control points identified during the tests are as follows:

1. 0.33 f'_m represents the point up to which the stress-strain curve remains linear. Thereafter, several cracks start developing in masonry introducing nonlinearity;
2. 0.75 f'_m is where vertical splitting cracks in bricks start developing at about this stress; however masonry still resists loads without much deterioration;
3. 0.9 f'_m represents the stress level in masonry just before the failure when the vertical splitting cracks propagate excessively throughout the masonry;
4. f'_m is the ultimate stress level in masonry after which the

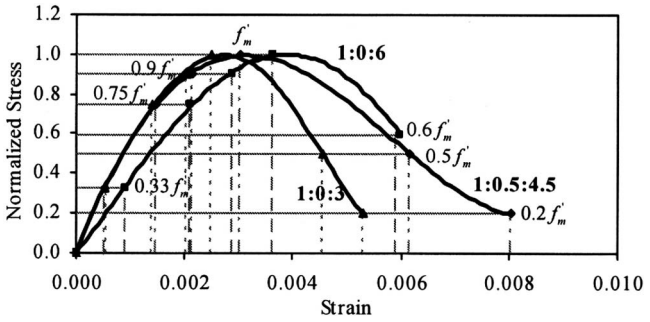

Stress in terms of f_m'	Strain in prism for mortar grades		
	1:0:6	1:0:3	1:0.5:4.5
0.00	0.0000	0.0000	0.0000
0.33	0.0009	0.0005	0.0005
0.75	0.0021	0.0014	0.0015
0.90	0.0029	0.0021	0.0021
1.00	0.0036	0.0025	0.0030
0.60	0.0059	-	-
0.50	-	0.0045	0.0062
0.20	-	0.0053	0.0080

Fig. 8. Stress-strain curves for masonry prisms for different grades of mortar: stress is normalized with respect to prism compressive strength for each curve

masonry begins to drop the load and exhibits sudden increase in the strains;

5. 0.5 f_m': the stress corresponding to this control point on the descending curve may be considered as the maximum dependable compressive strength of masonry; and
6. 0.2 f_m' is the maximum residual compressive stress and corresponding failure strain observed in masonry.

The last two control points were not recorded in the masonry prisms with weak mortar because of reasons already mentioned. These control points can be effectively used to define the performance limit states of the masonry material or member.

Analytical Model for Stress-Strain Curves of Masonry

Estimation of Prism Strength of Masonry

f_m' is the intrinsic property of masonry which can be used in the design of a variety of masonry elements, particularly the walls. f_m' is also used to estimate E_m and for plotting the masonry stress-strain curves. Therefore, f_m' is one of the most basic and required properties that must always be available for a given masonry. However, it is not always feasible to conduct compression testing of masonry prisms. On the other hand, f_b and f_j are readily available in the design codes or can be obtained easily by conducting tests. The three compressive strengths can be conveniently related as done in Eurocode6 (CEN 1996) as

$$f_m' = K f_b^{\alpha} f_j^{\beta} \tag{7}$$

where K, α, and β=constants. In addition, a few other factors have also been specified which take care of size and shape of bricks, dry strength of brick, "normalized" strength of bricks, etc.

As already discussed, f_m' does not depend upon the mortar strength as much as it does on the brick strength, therefore α must be higher than β. In Eurocode6 (CEN 1996), the values of α and β have been specified as 0.65 and 0.25, respectively, and K varies from 0.4 to 0.6 depending upon brick properties and brick–mortar joint configuration. These values of α and β are valid for mortar having compressive strength not more than 20 MPa or two times f_b, whichever is less.

Based on regression analysis of data obtained in an experimental study, Dayaratnam (1987) proposed different values of the constants K, α, and β as per the following equation

$$f_m' = 0.275 f_b^{0.5} f_j^{0.5} \tag{8}$$

Using experimental results on hollow structural clay tiles, Bennett et al. (1997) suggested that the masonry prism strength can be conservatively estimated as three-tenths of the brick compressive strength. Based on testing of solid clay brick masonry, the following equation is proposed by MSJC (2002) for estimating the masonry compressive strength

$$f_m' = A(400 + B f_b)(\text{psi}) \tag{9}$$

where A=1.0 for inspected masonry; and B varies from 0.2 to 0.25 for different mortar grades. The units of f_b in Eq. (9) are psi (1 MPa≈145 psi).

When the Eurocode6 (CEN 1996) relation, Eq. (7), is applied with K=0.6 (Group 1 bricks as per the code) to the present data, R^2 and σ come out to be 0.69 and 1.02 MPa, respectively ($0.8 f_b$ was used as the normalized strength of bricks). On the other hand, the relation proposed by Dayaratnam (1987), Eq. (8), gives a poorer match with R^2 value of −0.4 and σ value of 2.18 MPa. Clearly, equal weightage given to f_b and f_j (α=β=0.5) in Eq. (8) is not supported by this study. Similarly, since the expression suggested by Bennett et al. (1997) depends upon the compressive strength of brick units only, R^2 comes out to be poor (−0.19) and σ comes out to be much higher (2.01 MPa). Again, a poorer match results with the R^2 value of −0.21 and the σ value of 2.03 MPa when Eq. (9), proposed by MSJC (2002), is applied with B equal to 0.2 to the present data.

R^2 is the *coefficient of determination* between the experimentally obtained values and values obtained by regression analysis and σ is the *standard error of estimate*, which gives an idea of the scatter of actual data from the value estimated by regression analysis. A value of R^2 close to unity indicates a good fit and that close to zero indicates a poor fit, whereas it is desirable that σ is a minimum, implying that the scatter in the data about the estimated value is a minimum. R^2 and σ are calculated as (Wesolowsky 1976; Wonnacott and Wonnacott 1972)

$$R^2 = 1 - \frac{\sum (f_i - \hat{f}_{Ri})^2}{\sum (f_i - \bar{f})^2} \tag{10}$$

and

$$\sigma = \sqrt{\frac{\sum (f_i - \hat{f}_{Ri})^2}{n-3}} \tag{11}$$

where f_i and $\hat{f}_{Ri}$=ith experimentally obtained and regression estimated prism strength, respectively, $\bar{f}$=mean of the experimentally obtained prism strengths; and n=total number of data points. The divisor ($n-3$) is used in Eq. (11) rather than n in order to make an unbiased estimation of σ since three estimators (K, α, and β) are required in the σ calculation.

In the present study, K, α, and β have been obtained as 0.63, 0.49, and 0.32, respectively, by unconstrained regression analysis

Table 4. Comparison of past Experimental Results on Masonry Prisms with Analytical Predictions

	Experimental values (MPa)			Predicted values of f'_m (MPa)				
Research[a]	f_b	f_j	f'_m	Present study Eq. (12)	Eurocode6 (CEN 1996)	Dayaratnam (1987)	Bennett et al. (1997)	MSJC (2002)
Sarangpani 1	8.2	3.1	2.3	2.5 {10.3}[b]	2.7 {17.6}	1.4 {65.9}	2.5 {7.0}	4.4 {91.2}
Tomaževič	10.0	0.5	2.0	1.6 {28.2}	2.3 {12.7}	0.6 {225.2}	3.0 {50.0}	4.8 {137.9}
Sarangpani 2	10.7	4.1	2.9	3.2 {9.0}	3.4 {18.9}	1.8 {59.2}	3.2 {10.7}	4.9 {68.9}
Sarangpani 2	10.7	10.6	3.2	4.3 {33.6}	4.4 {36.2}	2.9 {9.6}	3.2 {0.0}	4.9 {52.9}
Naraine	13.1	6.1	5.4	4.0 {36.2}	3.6 {49.2}	2.5 {119.7}	3.9 {37.4}	5.4 {0.4}
Tomaževič	15.0	2.5	2.5	3.2 {27.4}	4.4 {75.5}	1.7 {48.5}	4.5 {80.0}	5.8 {130.3}
Rai[c]	17.0	9.9	7.3	5.3 {38.8}	5.8 {25.7}	3.6 {104.6}	5.1 {43.1}	6.2 {18.5}
Present	20.8	3.1	4.1	4.0 {2.4}	5.0 {20.8}	2.2 {85.7}	6.2 {52.2}	6.9 {68.7}
Present	20.8	15.2	6.6	6.7 {0.9}	7.4 {11.6}	4.9 {35.0}	6.2 {5.8}	6.9 {4.8}
Present	20.8	20.6	7.5	7.3 {2.2}	—[d]	5.7 {31.8}	6.2 {20.2}	6.9 {8.4}
Hendry	25.5	15.2	9.3	7.4 {26.4}	7.0 {32.7}	5.4 {71.8}	7.7 {21.6}	7.9 {18.3}
Binda	26.9	12.7	14.5	7.1 {103.3}	6.7 {117.9}	5.1 {185.3}	8.1 {79.7}	8.1 {78.2}
Ewing	34.0	15.7	15.6	8.6 {82.3}	9.4 {66.4}	6.4 {145.5}	10.2 {52.9}	9.6 {63.2}
McNary	101.7	3.4	29.9	9.0 {232.2}	14.2 {110.3}	5.1 {484.7}	30.5 {2.0}	23.1 {29.4}
McNary	101.7	13.7	32.5	14.0 {131.8}	20.1 {61.4}	10.3 {216.6}	30.5 {6.5}	23.1 {40.7}
McNary	101.7	26.4	40.9	17.3 {136.5}	—[d]	14.2 {187.0}	30.5 {34.1}	23.1 {77.1}
McNary	101.7	52.6	48.2	21.6 {123.6}	—[d]	20.1 {139.6}	30.5 {58.0}	23.1 {108.7}

[a]Sarangpani 1=Sarangapani et al. (2002), Tomaževič=Tomaževič (1999), Sarangapni 2=Sarangapani et al. (2005), Naraine=Naraine and Sinha (1989), Rai=Rai and Goel (1996), Hendry=Hendry (1998), Binda=Binda et al. (1988), Ewing=Ewing and Kowalsky (2004), McNary=McNary and Abrams (1985).

[b]Figures in the { } bracket indicate the percent error between the experimental and predicted values.

[c]Reclaimed bricks from about 100 years old building in North America and 1:1:6 mortar were used in prisms.

[d]Eurocode6 (1996) is applicable only for masonry with mortar strength less than 20 MPa.

of Eq. (7) using the least-square fit method, and the following equation is proposed, which gives the R^2 and σ as 0.93 and 0.48 MPa, respectively, for the present data

$$f'_m = 0.63 f_b^{0.49} f_j^{0.32}; \quad (R^2 = 0.93,\ \sigma = 0.48\ \text{MPa}) \tag{12}$$

Eq. (12) is used to estimate the masonry prism compressive strength from the compressive strengths of bricks and mortar obtained experimentally in nine different published studies in the past (Sarangapani et al. 2002; Tomaževič 1999; Sarangapani et al. 2005; Naraine and Sinha 1989; Rai and Goel 1996; Hendry 1998; Binda et al. 1988; Ewing and Kowalsky 2004; McNary and Abrams 1985). The prism strengths predicted by Eq. (12) are compared with those obtained using four different analytical relations proposed by Eurocode6 (CEN 1996), Dayaratnam (1987), Bennett et al. (1997), and MSJC (2002). Table 4 shows that the proposed equation is fairly good in predicting the prism compressive strength with error in the range of 1–40%, except in the case of prisms made with high strength bricks. Equations proposed by Eurocode6 (CEN 1996), Bennett et al. (1997), and MSJC (2002) are good for masonry constructed with high strength bricks, however for lower strength bricks, the error in estimating the masonry compressive strength is comparatively higher. The relation proposed by Bennett et al. (1997) depends on the compressive strength of brick units only; therefore it does not take care of weakness induced in masonry because of the use of low strength mortars. The equation proposed by Dayaratnam (1987) gives equal weight to the compressive strengths of bricks and mortar, therefore in most of the cases, the errors in estimation of masonry compressive strength is higher.

The estimation of masonry compressive strength using Eq. (12) proposed in the present study is consistently better for prisms made with low and average strength bricks. However for prisms made with high strength bricks (more than ~25 MPa), the estimation done by Bennett et al. (1997) is much better.

Estimation of Peak Strain of Masonry

It has been observed in the present study that the ascending part of the masonry stress-strain curve can be represented by a parabolic curve which provides a good fit to the experimental data as observed by Paulay and Priestley (1992), Sawko and Rouf (1984), and Priestley and Elder (1983). The parabolic variation can be expressed in nondimensional form in terms of stress ratio and strain ratio as

$$\frac{f_m}{f'_m} = 2\frac{\varepsilon_m}{\varepsilon'_m} - \left(\frac{\varepsilon_m}{\varepsilon'_m}\right)^2 \tag{13}$$

where f_m and ε_m=compressive stress and strain in masonry, respectively; and ε'_m=peak strain corresponding to f'_m. Further, the parabolic curve can be extended in the descending part of the stress-strain curve until f'_m drops to 90%; the corresponding strain can be calculated using Eq. (13). After the stress level of 0.9 f'_m is reached on the descending part, the curve can be simplified as a straight line up to the residual stress in masonry, i.e., 20% of f'_m. A problem remains in estimating the value of ε'_m for the masonry prism in field applications because it is difficult and cumbersome to do the controlled tests with accurate measuring instruments and loading machines. In the present study, the following equation is proposed to estimate ε'_m by regression analysis of the experimental data.

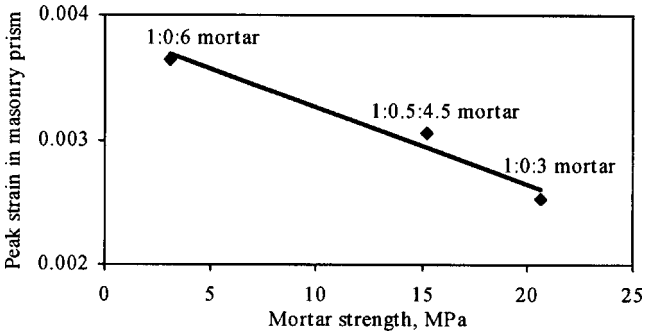

Fig. 9. Dependence of masonry strain on mortar strength

$$\varepsilon'_m = C_j \frac{f'_m}{E_m^{0.7}}; \quad \{R^2 = 0.83, \sigma = 0.0001\} \tag{14}$$

where C_j=factor depending upon the strength of mortar used in prism given by

$$C_j = \frac{0.27}{f_j^{0.25}} \tag{15}$$

It is observed in the present study that peak strain in masonry prisms reduces with increase in mortar strength (Fig. 9) and this effect must be included while estimating the peak strain. Although, the effect of mortar strength has already been included in Eq. (12), which estimates the prism strength, weightage given to f_j was obviously less because prism strength is influenced more by the brick strength. However, the deformation characteristics of masonry are dominated by the weaker and softer component, i.e., mortar; therefore C_j is incorporated in Eq. (14).

As shown in Fig. 10, Eqs. (12)–(15) can be used to plot the ascending parabolic masonry stress-strain curve from origin up to $\{\varepsilon'_m, f'_m\}$ and then the parabolic variation can be extended in the descending part up to the point corresponding to 0.9 f'_m. Thereafter, the linear descending part follows, joining the point corresponding to 0.9 f'_m to $\{2\varepsilon'_m, 0.2f'_m\}$ for mortar without any lime content, and to $\{2.75\varepsilon'_m, 0.2f'_m\}$ for mortar with lime content. In the present study, lime content in mortar was fixed such that the total of cement and lime content remains three times the sand content. A higher failure strain value is proposed for masonry with lime mortar because lime introduces ductility in the masonry.

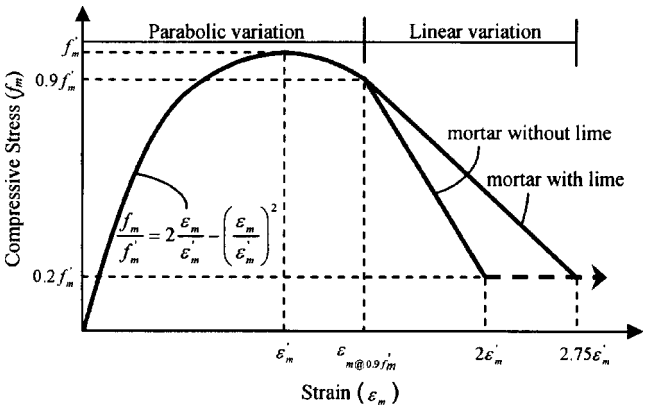

Fig. 10. Idealized stress-strain relationship for masonry

Fitness of Proposed Analytical Model

The proposed analytical model for compressive stress-strain curves is examined for its fitness by comparing it with: (1) experimental curves obtained in the present study; (2) experimental curves obtained in seven different studies published in the past (Sarangapani et al. 2002; Naraine and Sinha 1989; Rai and Goel 1996; Hendry 1998; Binda et al. 1988; Ewing and Kowalsky 2004; Sawko and Rouf 1984); and (3) analytical curves generated using two different models suggested by Priestley and Elder (1983) and Eurocode6 (CEN 1996). The analytical model suggested by Priestley and Elder (1983) does not propose any relation to estimate f'_m, therefore experimental values of f'_m are required in generating the stress-strain curves. However, analytical relations for estimating f'_m have been proposed by Eurocode6 (CEN 1996) and in the present study. Therefore for better comparison among the three analytical models, stress-strain curves are generated using: (i) predicted f'_m; and (ii) experimentally obtained f'_m.

A comparison of stress-strain curves generated by the present analytical model with those obtained in the present experimental study is shown in Figs. 11(a–c), which show a very close match between the analytical and experimental curves. f'_m predicted by the present analytical model match really well their experimental counterparts (Table 4). Therefore, Figs. 11(a–c) show the curves generated by the present analytical model using only the predicted f'_m.

Stress-strain curves have been generated by the proposed model using f_b and f_j reported in the past seven experimental studies and compared with the experimental curves of the original studies in Figs. 11(d–j). The proposed analytical model clearly demonstrates a reasonably good prediction of the stress-strain curves when compared with the experimental curves. The proposed model successfully predicts prism strengths and corresponding peak strain values fairly accurately. In most of the cases, failure strains predicted by the proposed model are significantly greater than the corresponding experimental values. This may be due to the fact that it is difficult to record the rapidly descending part of the stress-strain curves experimentally and, therefore, the researchers of these studies may not have accurately recorded the diminishing curve. Sarangapani et al. (2002) used very soft and weak bricks in their experimental study, therefore prism strength reported in their study is also much less, which matches quite well with their predicted values based on the present study [Fig. 11(d)]. For all other studies in which high strength bricks were used, predicted prism strengths are observed to be less than their experimental counterparts.

Experimental stress-strain curves of the present study and the seven past studies are also compared with the analytical estimation using the two past models: the "modified" Kent–Park model proposed by Priestley and Elder (1983), and the Eurocode6 (CEN 1996) idealized model. Figs. 11(a–j) show that for most of the cases, these two analytical models predict significantly stiffer stress-strain curves. The formulation of the Priestley and Elder (1983) model is such that for weaker mortar (f_j less than ~7 MPa), the descending branch of the stress-strain curve cannot be predicted, while for the other two mortar grades it predicts fairly good failure strain values. The Eurocode6 (CEN 1996) model simply plateaus after reaching the prism strength, and the recommended peak strain and failure strain values are significantly less than those of the experimental values.

Fig. 11 shows that the analytical model proposed in the present study is fairly good when experimental prism strengths are used

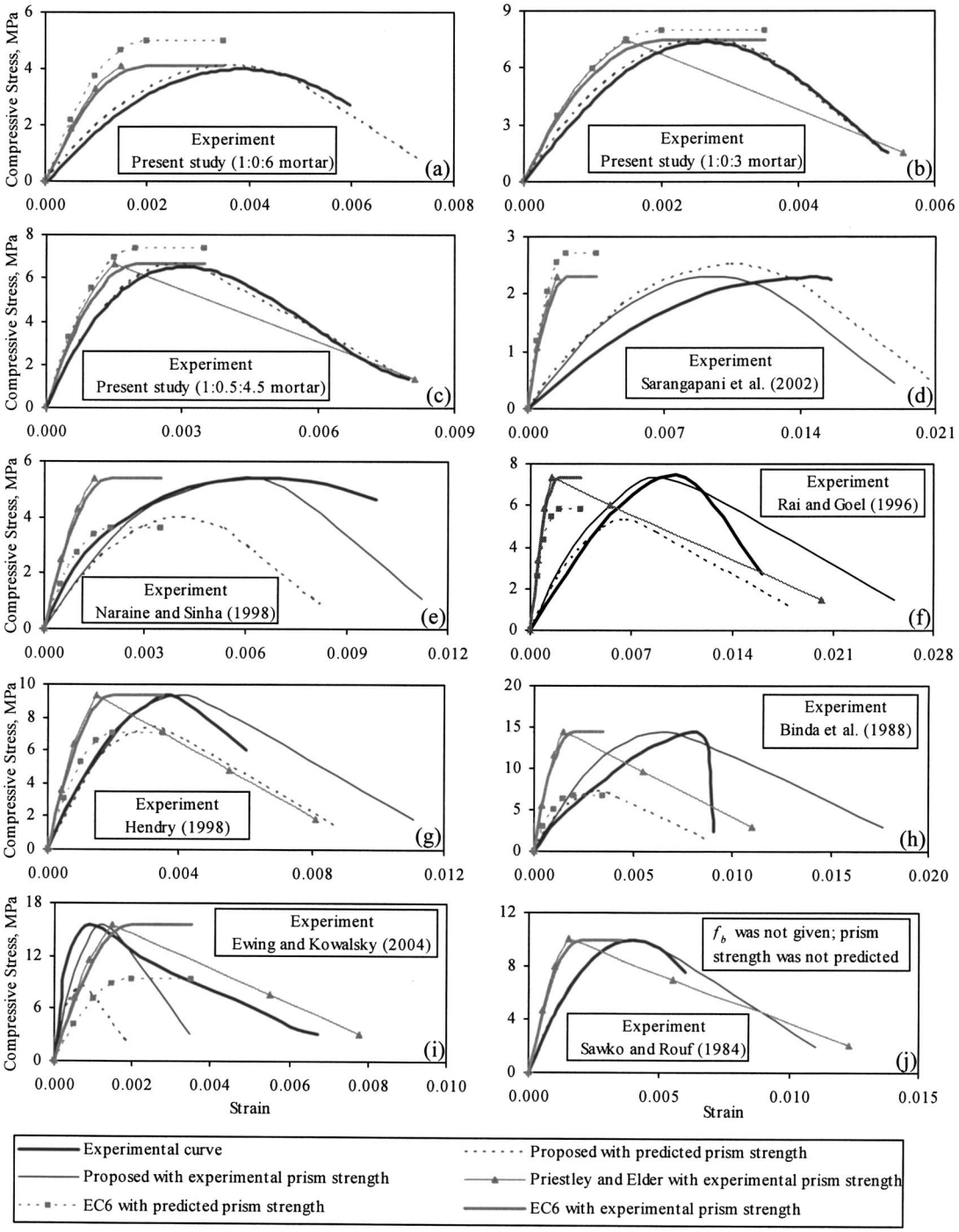

Fig. 11. Comparison of stress-strain curves of masonry estimated by proposed analytical model and models of other researchers with experimental curves obtained in several published studies

and consistently better than the other two analytical models because of its simplicity and fitness. The present analytical model can be conveniently used in the analysis and design procedures of masonry elements.

Conclusions

The objective of the research was to investigate experimentally the compressive behavior of masonry and its constituents and to develop the stress-strain curves. The relation between brick, mortar, and masonry strengths and the effects of other factors, such as water absorption, initial rate of absorption, and addition of lime in the mortar on the strength and ductility of masonry were also studied.

IRA was found to be more directly related to the compressive strength of bricks than WA. The compressive strengths of bricks with lower values of IRA were observed to be significantly higher. A much better *correlation coefficient* was found between IRA and compressive strength (−0.77) than that for WA and compressive strength (−0.24). Therefore, IRA tests for bricks should be made mandatory by the national codes.

Simple relations are suggested to estimate the modulus of elasticity of bricks, mortar, and masonry as 300, 200, and 550 times their compressive strengths, respectively. Masonry prism compressive strength was found to increase with increase in compressive strengths of bricks and mortar. However, increase in masonry strength was more prominent in the case of masonry constructed with weaker mortar. Therefore, using a higher strength mortar than required is unlikely to produce higher strength masonry.

Stress-strain curves of masonry constructed with bricks and mortar of comparable strengths and stiffness was observed to lie below the stress-strain curves of both bricks and mortar, which is not in accordance with the generally accepted compressive behavior of masonry. Therefore, more experimental study is required with different combinations of brick types and mortar grades to develop a generalized model for compressive behavior of masonry.

Compressive behavior of mortar with lime was found to be better because of greater ductility; failure strain was about 45% more than that for *strong* mortar although the compressive strength was about 35% less. For the same reasons, compressive behavior of masonry with lime mortar was found to be much better than that of masonry with limeless mortar; failure strain was about 50% greater and prism strength only about 13% less than those for prisms with *strong* mortar. Adding lime in mortar is a very old practice in many parts of the world, including India; however some national codes, e.g., IS1905 (IS 1987) and Eurocode6 (CEN 1996), allow the use of limeless mortars; which this research indicates may not be a good construction practice.

Six control points were identified on the compressive stress-strain curves of masonry, which correspond to the experimentally observed six *significant* events representing compressive stresses in masonry and the corresponding strains. The control points can also be used as performance limit states for masonry material and member. Based on these control points, an analytical model was developed by regression analysis of the experimental data to plot the masonry stress-strain curves, which follow a combination of parabolic and linear variation. The analytical model is really simple since it requires only two inputs: brick compressive strength and mortar compressive strength. The model estimates fairly good stress-strain curves when compared with several experimental and analytical research works published in the literature. Therefore, it can be conveniently used in the analysis and design procedures of masonry elements. Conclusions made in the present study may change based on different combinations of cement, lime, sand, and water used in brickwork.

Acknowledgments

The writers gratefully acknowledge the help extended by Dr. K. K. Bajpai, Mr. Uma Mahesh Reddy, and the staff at the Structural Engineering Laboratory at IIT Kanpur in conducting the experiments. The financial assistance provided by the Ministry of Human Resource Development (MHRD), Government of India, is gratefully acknowledged.

Notation

The following symbols are used in this paper:

A, B = constants depending upon state of masonry and mortar grade, respectively;
C_j = factor related to compressive strength of mortar;
C_r = correlation coefficient;
COV = coefficient of variation;
E_b = modulus of elasticity of bricks (MPa);
E_j = modulus of elasticity of mortar (MPa);
E_m = modulus of elasticity of masonry (MPa);
$\bar{f}$ = mean of the experimentally obtained masonry prism strengths (MPa);
f_b = compressive strength of bricks (MPa);
f_i = ith experimentally obtained masonry prism strength (MPa);
f_j = compressive strength of mortar (MPa);
f_m = compressive stress in masonry (MPa);
f'_m = compressive prism strength of masonry (MPa);
$\hat{f}_{Ri}$ = regression estimated masonry prism strength (MPa);
K = constant depending upon brick properties and brick-mortar joint configuration;
n = total number of data points;
R^2 = coefficient of determination;
Z_m = factor depending upon compressive strength of mortar;
α, β = constants representing contribution of bricks and mortar compressive strengths on f'_m;
ε_m = compressive strain in masonry;
ε'_m = peak strain in masonry, i.e., compressive strain corresponding to f'_m; and
σ = standard error of estimate (MPa).

References

ASTM. (2001a). "Standard test method for compressive strength of hydraulic cement mortars (using 2-in or 50-mm cube specimens)." *Masonry test methods and specifications for the building industry, ASTM C 109/C 109M-99*, 4th Ed., Philadelphia.

ASTM. (2001b). "Standard test method for compressive strength of masonry prisms." *Masonry test methods and specifications for the building industry, ASTMC 1314-00a*, 4th Ed., Philadelphia.

ASTM. (2001c). "Standard test methods for sampling and testing brick and structural clay tile." *Masonry test methods and specifications for the building industry, ASTM-C67-00*, 4th Ed., Philadelphia.

Atkinson, R. H., and Noland, J. L. (1983). "A proposed failure theory for brick masonry in compression." *Proc., 3rd Canadian Masonry Symp.*, Edmonton, Alta., Canada, 5.1–5.17.

Bennett, R. M., Boyd, K. A., and Flanagan, R. D. (1997). "Compressive properties of structural clay tile prisms." *J. Struct. Eng.*, 123(7), 920–926.

Binda, L., Fontana, A., and Frigerio, G. (1988). "Mechanical behaviour of brick masonries derived from unit and mortar characteristics." *Proc., 8th Int. Brick and Block Masonry Conf.*, Vol. 1, Dublin, Ireland, 205–216.

Canadian Standards Association (CSA). (2004). *Design of masonry structures, S304.1*, Ontario, Canada.

Dayaratnam, P. (1987). *Brick and reinforced brick structures*, Oxford and IBH, New Delhi, India.

Drysdale, R. G., Hamid, A. A., and Baker, L. R. (1994). *Masonry structures: Behaviour and design*, Prentice-Hall, Englewood Cliffs, N.J.

European Committee of Standardization (CEN). (1996). "Design of masonry structures. Part 1-1: General rules for buildings—Reinforced and unreinforced masonry." *ENV 1996-1-1*, *Eurocode 6*, Brussels, Belgium.

Ewing, B. D., and Kowalsky, M. J. (2004). "Compressive behavior of unconfined and confined clay brick masonry." *J. Struct. Eng.*, 130(4), 650–661.

Federal Emergency Management Agency (FEMA). (1999). *Evaluation of earthquake damaged concrete and masonry wall buildings, basic procedures manual, ATC-43*, FEMA 306, Applied Technology Council, Calif.

Grimm, C. T. (1975). "Strength and related properties of brick masonry." *J. Struct. Div.*, 101(1), 217–232.

Hendry, A. W. (1998). *Structural masonry*, 2nd Ed., Macmillan, London.

International Code Council. (2003). *International building code*, Va.

Indian Standards (IS). (1987). *Indian standard code of practice for structural use of unreinforced masonry, IS1905*, 3rd Rev., Bureau of Indian Standards, New Delhi, India.

Indian Standards (IS). (1992a). *Indian standard methods of test of burn clay building bricks—Part 1: Determination of compressive strength, IS 3495*, 3rd Rev., Bureau of Indian Standards, New Delhi, India.

Indian Standards (IS). (1992b). *Indian standard methods of test of burn clay building bricks—Part 2: Determination of water absorption, IS 3495*, 3rd Rev., Bureau of Indian Standards, New Delhi, India.

Indian Standards (IS). (1995). *Indian standard code of practice for preparation and use of masonry mortars, IS2250*, 5th Rev., Bureau of Indian Standards, New Delhi, India.

Masonry Standards Joint Committee (MSJC). (2002). *Building code requirements for masonry structures, ACI 530-02/ASCE 5-02/TMS 402-02*, American Concrete Institute, Structural Engineering Institute of the American Society of Civil Engineers, The Masonry Society, Detroit.

McNary, W. S., and Abrams, D. P. (1985). "Mechanics of masonry in compression." *J. Struct. Eng.*, 111(4), 857–870.

Naraine, K., and Sinha, S. (1989). "Behavior of brick masonry under cyclic compressive loading." *J. Struct. Eng.*, 115(6), 1432–1445.

Paulay, T., and Priestley, M. J. N. (1992). *Seismic design of reinforced concrete and masonry buildings*, Wiley-Interscience, New York.

Priestley, M. J. N., and Elder, D. M. (1983). "Stress-strain curves for unconfined and confined concrete masonry." *ACI J.*, 80(3), 192–201.

Rai, D. C., and Goel, S. C. (1996). "Seismic strengthening of unreinforced masonry piers with steel elements." *Earthquake Spectra*, 12(4), 845–862.

Sarangapani, G., Venkatarama Reddy, B. V., and Jagadish, K. S. (2002). "Structural characteristics of bricks, mortar and masonry." *J. Struct. Eng. (India)*, 29(2), 101–107.

Sarangapani, G., Venkatarama Reddy, B. V., and Jagadish, K. S. (2005). "Brick-mortar bond and masonry compressive strength." *J. Mater. Civ. Eng.*, 17(2), 229–237.

Sawko, F., and Rouf, M. A. (1984). "On the stiffness properties of masonry." *Proc. Inst. Civ. Eng., Part 2. Res. Theory*, 77, 1–12.

Tomaževič, M. (1999). *Earthquake-resistant design of masonry buildings*, Imperial College Press, London.

Wesolowsky, G. O. (1976). *Multiple regression and analysis of variance*, Wiley, New York.

Wonnacott, T. H., and Wonnacott, R. J. (1972). *Introductory statistics for business and economics*, Wiley, New York.